Asian Journal of Information Technology 15 (5): 855-861, 2016
ISSN: 1682-3915
© Medwell Journals, 2016

Reduction of FBM Noise in Brain MRI Images Using Wavelet Thresholding Techniques

N. Rajeswaran and C. Gokilavani
Department of ECE, Malla Reddy Engineering College, Seunderabad, Telangana, India

Abstract: In medical image processing, noise plays a role of reducing the details of the images and blurs the features which are important for the diagnosis of the disease. Brain images are fractal in nature and especially in brain MRI (Magnetic Resonance Imaging) images, fractional Brownian motion (fBm) noise affects the important features. To reduce the effect of fBm noise in brain MRI images by implementing wavelet based thresholding techniques namely visu shrink, SURE shrink and bayes shrink and to compare the performance of these techniques using various evaluation metrics. The fBm noise is greatly reduced in bayes shrink and it has high values of PSNR. This study provides, the implementation of wavelet domain thresholding techniques for denoising brain MRI images and provides a comparison of these shrink methods using PSNR (Peak Signal to Noise Ratio), MSE (Mean Square Error), absolute error, fractal dimension, IEF (Image Enhancement Factor), normalized cross correlation, structural content and much more.

Key words: Bayes shrink, fbm noise, fractal dimension, IEF, medical image processing, MSE, normalized cross correlation, PSNR, structural content, SURE shrink, visu shrink, wavelet thresholding

INTRODUCTION

In medical image processing, noise tends to reduce the visibility of the image and obscures the information needed for accurate treatment. Since, the larger part of image processing deals with Image restoration or image denoising, denoising the noise affected images plays a major role to diagnose the diseases in a proper manner and to retain the image up to its quality (Al-Kadi, 2010; Chicklore *et al*., 2013). Image denoising attempts to remove the various types of noises present in an image and restores the original image back while preserving the important features needed for proper diagnosis and to track the progress of the disease. Image denoising finds application in various fields such as astronomy, forensic science and so on. Also, the tradeoff between the image features and noise reduction must be taken into account while denoising. Recently, fuzzy logic has been used for noise removal Farbiz *et al*., 2000). Medical images are taken by means of MRI (Magnetic Resonance Iimaging), CT (Computed Tomography) and ultrasound imaging. Each of these methods has their own advantages and disadvantages. Among these MRI sounds better in giving high resolution images of the soft tissues in human body. Human brain is the soft and most complex organ of human body. An image of human brain consists of several complex patterns that are independent of scales. Thus brain image is a self similar structure and is fractal in nature (Liu *et al*., 2007; Gevers and Smeulders, 2000).

Various types of noises are present in brain MRI images. They include salt and pepper noise, Gaussian noise, speckle noise and fractional brownian motion noise (fBM noise). This fBM noise is caused by the brownian motion. Brownian motion deals with uncertainty in movement of particles and the theory which combines the concept of fractals and brownian motion is called fBm (fractional Brownian motion).The noise due to fBm noise is called fBm noise. This noise is caused by random movement of tiny particles that are suspended in the brain fluid and it greatly affects the brain MRI images (Le Bihan, 2003).

MATERIALS AND METHODS

Wavelet based thresholding techniques: Recently, in all fields of science DWT (Discrete Wavelet Transform) is the emerging trend and it applies well to image processing. Wavelet transform has excellent localization property and it has been an inherent tool in image denoising and image compression. We can represent an image with high resolution with sparsity. Wavelet denoising removes the noise present in an image and it preserves the image details without considering the frequency content of the image and so, it suits well for medical images. In DWT, the image is considered to be consisting of small functions called wavelets. The important properties of wavelet transform that are considered while denoising an image are multiresolution, sparsity and edge detection and clustering.

Corresponding Author: N. Rajeswaran, Department of ECE, Malla Reddy Engineering College, Seunderabad, Telangana, India

Thresholding is important to differentiate the useful pixels in an image with the redundant pixels. If the threshold value is large then many of the image details are destroyed. And, when it is chosen small, the noises are not properly removed. Wavelet thresholding attempts to remove noise based on the threshold value (Bala and Ertuzun, 2005). In general, there are two types of thresholding namely hard thresholding and soft thresholding. In hard thresholding, the pixels below the threshold are set to zero and the pixels above the threshold are set to one. In soft thresholding, the coefficients which are above the threshold are shrinked. The three steps that are involved in wavelet based denoising are:

- Computation of the forward wavelet transform
- Filtering wavelet coefficients using thresholding
- Computation of inverse wavelet transform

This study implements three thresholding techniques namely:

- Visu shrink
- SURE (Stein's Unbiased risk Estimator) shrink and
- Bayes shrink

Andria *et al.* (2013) suggests a new thresholding procedure for removing speckle noise in medical ultrasound images and uses a combination of Visu shrink SURE shrink and Bayes shrink to propose a new threshold (Hiremath *et al.*, 2013). This method uses the wavelet coefficients for suppressing the noise in the medical images and to reduce the amount of redundant coefficients. It also suppresses the disturbances due to noise and it preserves the features of the image.

Visu shrink: Here, fixed threshold (Xu *et al.*, 2014) is applied and is given by the equation:

$$T_u = \sigma_n^2\sqrt{2\log N.} \tag{1}$$

Where N is the size of the image and the median absolute deviation of noise ó$_n^2$ is given by:

$$\sigma_n^2 = \left[\frac{\text{median}\left(\text{HH1}(n,m)\right)}{0.6745}\right]^2 \tag{2}$$

Here, n and m are the pixel indices of the sub band HH1 (Hu *et al.*, 2012) which is obtained by the first level of wavelet decomposition. Visu shrink considers only the images of size N and the standard deviation of the noise. Visu shrink threshold value increases as the number of pixels in the image increase and as a result, the significant coefficients are killed. Visu shrink minimizes the overall error in the denoised image and produces overly smoothened estimation. This method does not work properly if there are discontinuities in the signal.

Sure shrink: The combination of universal threshold and the stein's unbiased risk estimator constitutes SURE shrink. Here, there is separate threshold for each sub-band (Andria, *et al.*, 2013). This is best suited to image with sharp discontinuities. This performs well in denoising the image and it has minimum value for mean square error. The threshold function is given by:

$$T_S = \min\left(T\sigma_n^2\sqrt{2\log N}\right) \tag{3}$$

Here, T is the value that minimizes the Stein's unbiased risk estimator.

Bayes shrink: Bayes shrink models the wavelet coefficients with general gaussian distribution. This adapts to both signal and noise characteristics. The threshold is given by the relation:

$$T_b = (\sigma_x) = \frac{\sigma_n^2}{\sigma_x} \tag{4}$$

Here, σ_x denotes the standard deviation of the image in each wavelet sub band.

Generation of fbm noise: Based on the concept of bisection and interpolation (Penttinen and Virtamo, 2005) ilkka norros proposed the simulation of fractional brownian motion with conditional random midpoint displacement algorithm. The fractional brownian motion is generated by using random mid-point displacement algorithm. This is also called as diamond square algorithm. This produces fractals in images.

This RMD (Random Mid-point Displacement) algorithm (Minnie and Srinivasan, 2014.) requires prior length of simulation to produce the fractional Brownian motion. Here, the entire trace of the fractional brownian motion is generated before it is used for the purpose for which it is specified for. Fractional brownian motion has been used in various fields such as hydrology, imaging landscapes and much more (Oigard *et al.*, 2005). The properties of a normalized fBm are:

- Normalized fBm is a stochastic process (Zt) with Hurst parameter, H(0,1)
- Zt has stationary increments
- Zt is Gaussian
- Zt has continuous sample paths

Ordinary brownian motion is the special case of normalized fBM with the parameter H = 1/2 (Hu *et al.*, 2012). This algorithm consists of following steps:

- Step 1: Take the given image
- Step 2: Assign height values to each corner of image

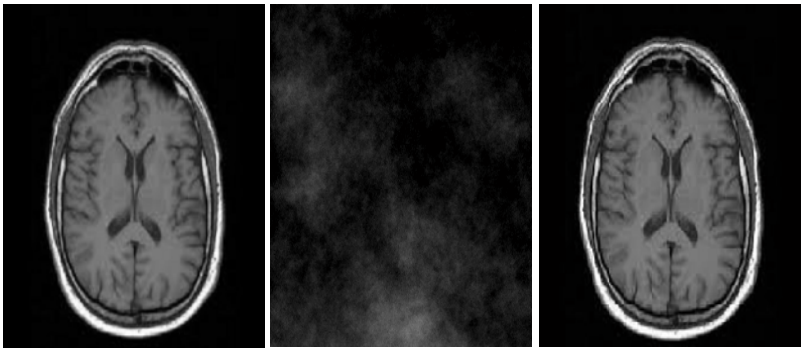

(a) (b) (c)

Fig. 1a-c): Simulation results of fractional brownian motion noise

- Step 3: Divide the image into four sub-images and assign height values to them such that their height is the mean values of the corners of the image taken in step 1
- Step 4: When computing the middle height, add small error value depending on the image size taken in step 1 and some constants that controls the fractal's roughness
- Step 5: Continue the iteration and sub-divide the sub-images further
- Step 6: When no noticeable difference is seen, stop the iteration and render the pixel with mean height values

Thus the fractals are produces by the above RMD procedure and are shown. Figure.1 shows the MATLAB simulation results for the generation of fractional brownian motion noise for an MRI image of size 512×512. Figure 1a shows the original brain MRI image. Figure 1b shows the pattern of fractional brownian motion. Figure 1c shows the brain MRI image corrupted with fBM noise.

Bayes shrink: The proposed approach aims at reducing the fBm noise using wavelet based thresholding techniques. Various techniques are proposed in the literature for the simulation of fractional brownian motion using wavelets and wavelet transform. Synthesis of fractional brownian motion has also been discussed and proposed in the literature based on wavelet transform. The flow chart for the proposed approach is given below and is based fully on thresholding in wavelet transform.

Figure 2, initially the original brain MRI image is taken and is given to the noise generation algorithm. This step leaves us a noisy image. This noisy image is subjected to wavelet decomposition (either 1 level or 2 levels). Then use the wavelet shrinkage techniques to calculate the threshold value. Apply, the threshold values

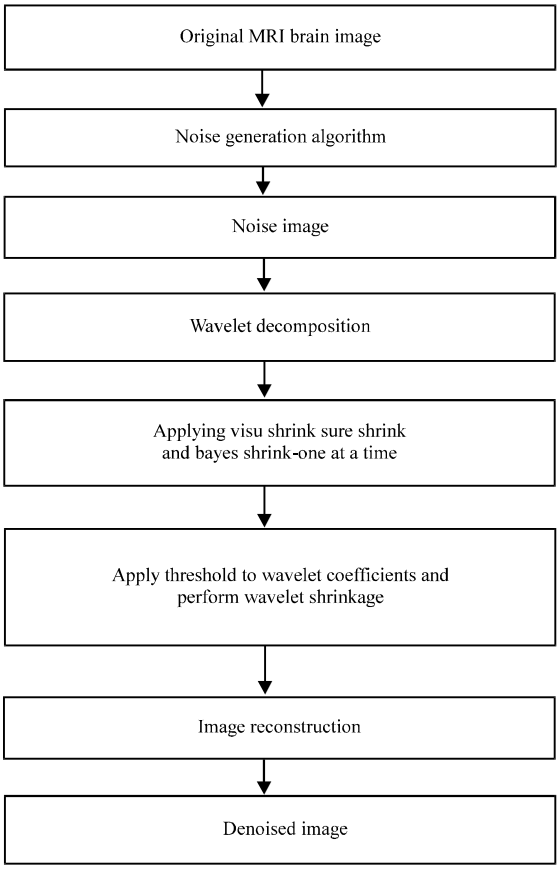

Fig. 2: Flow chart of the proposed approach

to the wavelet coefficients and perform wavelet shrinkage. In wavelet shrinkage all the coefficients are shrinked according to the threshold value. Then, the reconstructed image is formed with the help of the shrinked coefficients and thus, the denoised image is obtained.

Performance evaluation metrics: The performance (Minnie and Srinivasan, 2014.) of the denoising techniques is tested through various evaluation metrics

and their formulae are given below: The formula for MSE (Mean Square Error) is given by:

$$MSE = \frac{1}{MN}\sum_{j=1}^{M}\sum_{k=1}^{N}\left(x_{jk} - x_{jk}\right)^2 \quad (5)$$

The formula for PSNR (Peak to Signal Noise Ratio) is given by:

$$PSNR = 10\log\frac{(255)^{\wedge 2}}{MSE} \quad (6)$$

Where x_{jk} represents the original image and $x^{j,k}$ represents the restored image. The formula for Normalized Cross Correlation (NK) is given by:

$$NK = \sum_{jk}^{M}\sum_{ijk}^{N} x_{jk}x_{jk} / \sum_{jk}^{M}\sum_{jk}^{N} x_{jk}^2 \quad (7)$$

Where is the original image and is the denoised image. The formula for Average Difference (AD) is given by:

$$AD = \sum_{j=1}^{M}\sum_{k=1}^{N}\left(x_{j,k} - x_{j,k}\right) / MN \quad (8)$$

Where
$x_{j,k}$ The original image and
$x_1^{j,k}$ The denoised image.

The formula for Structural Content (SC) is given by:

$$SC = \sum_{J=1}^{M}\sum_{k=1}^{N} x_{j,k}^2 / \sum_{j=1}^{M}\sum_{k=1}^{N} x_{j,k}^2 \quad (9)$$

Where:
$x_{j,k}$ = The original image
x_{jk} = The denoised image.

The formula for Maximum Difference (MD) is given by:

$$MD = Max\left(\left|x_{j,k} - x_{j,k}\right|\right) \quad (10)$$

Where:
$x_{j,k}$ = The original image
$x_{j,k}$ = The denoised image.

The formula for Normalized Absolute Error (NAE) is given by:

$$NAE = \sum_{j=1}^{M}\sum_{k=1}^{N}\left|x_{j,k} - x_{j,k}\right| / \sum_{j=1}^{M}\sum_{k=1}^{N}\left|x_{j,k}\right| \quad (11)$$

Where:
$x_{j,k}$ = The original image
$x_{j,k}$ = the denoised image

The IEF (Image Enhancement Factor) is given by:

$$IEF = \frac{\text{Noisy image} - \text{Orignal image}}{\text{Denoise image} - \text{Orignal image}} \quad (12)$$

The SSIM (Structural Similarity Index) metric is calculated on various windows of an image. The measure between two windows x and y of common size N×N is:

$$SSIM(x,y) = \frac{\left(\mu_x\mu_y + C_1\right)\left(2\sigma_{xy} + C_2\right)}{\left(\mu_x\mu_y + C_1\right)\left(\sigma_x^2 + \sigma_y^2 C_2\right)} \quad (13)$$

Where:
μ_x = The average of x
μ_y = The average of y
$\sigma_x 2$ = The variance of x
$\sigma_y 2$ = The variance of y
σ_{xy} = The covariance of x and y
c_1 = $(K_1 L)^2$
c_2 = $(K_2 L)^2$
c_1, c_2 = Two variables to stabilize the division with weak denominator
L = The dynamic rangeof the pixel-values
K_1 = 0.01
K_2 = 0.03 by default

RESULTS AND DISCUSSION

The wavelet based thresholding techniques are implemented by using MATLAB (R2013a) and the simulation results for Visu shrink are given in Fig. 3. The Fig. 3a shows the original image. Figure 3b shows the noisy image. Figure 3c shows the denoised image. Here in the noisy image, the value of the hurst parameter is 0.3 (for a classical brownian motion, the hurst parameter h = 0.5).

The simulation results for SURE shrink are given in Fig. 4. Figure 4a shows the original image. Figure 4b shows the noisy image. Figure 4c shows the denoised image. Here, also the noisy image takes the value of 0.3 for H.

The simulation results for bayes shrink are given in Fig. 5. Figure 5a shows the original image. Figure 5b shows the noisy image (with hurst parameter of 0.3). Figure 5c shows the denoised image.

The performances of all the three thresholding techniques are listed in Table 1 (Figure 6-10 show the comparison graph for all the performance metrics for various samples of brain MRI images.

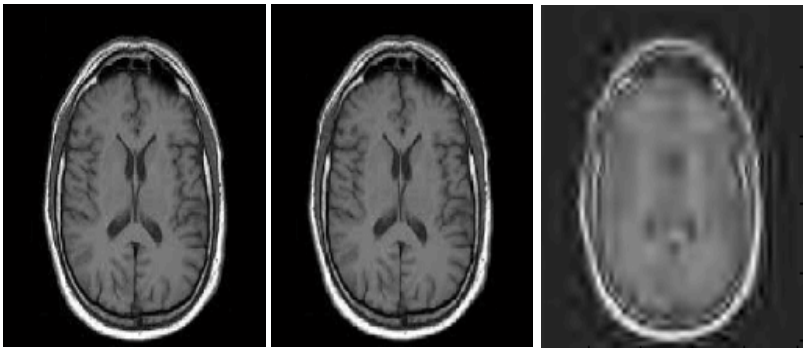

(a) (b) (c)

Fig. 3: Simulation results for visu shrink

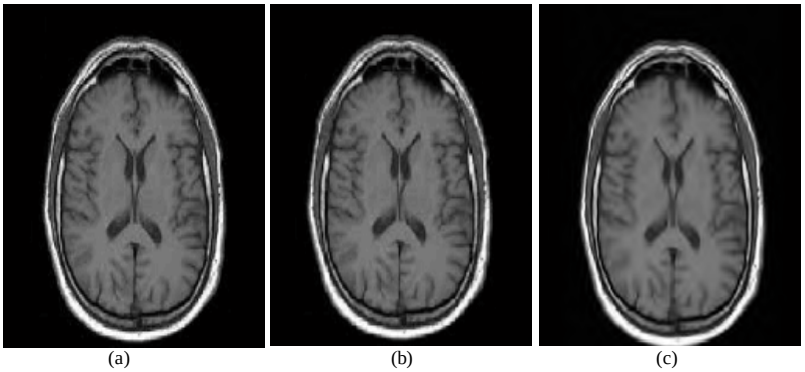

(a) (b) (c)

Fig.4: Simulation results for SURE shrink

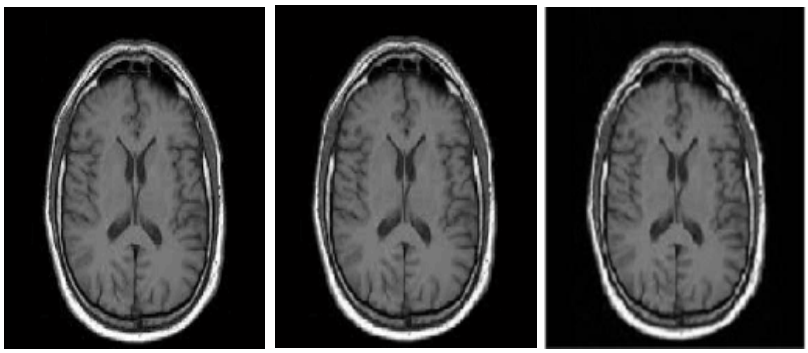

(a) (b) (c)

Fig. 5: Simulation results for bayes shrink

Table 1: Comparison of wavelet thresholding techniques

Performance metrics	Visu shrink	Sure shrink	Bayes shrink
MSE (Mean Square Error)	0.5499e+02	0.3632e+02	0.15e-02
PSNR (Peak signal to Noise ratio)	30.7295	32.5282	76.2524
FD (Fractal Dimension)	1.9915	1.9859	1.9852
IEF (Image Enhancement Factor)	1.0258	1.0299	9.3977
SSIM (Structural Similarity Index)	1.000	0.8452	1.000
NK (Normalized Cross Correlation)	0.7172	0.9984	0.9989
AD (Average Difference)	24.5535	0.0434	0.0559
SC (Structural Content)	1.3690	1.0011	1.0006
MD (Maximum Difference)	255	237	239
NAE (Normalized Absolute Error)	0.3975	0.0145	0.0032
Time elapsed when attempt to denoise (sec)	1.3604	8.7924	1.2801

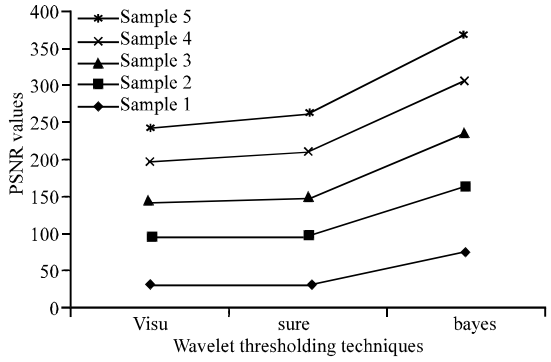

Fig. 6: Chart for Peak Signal to Noise Ratio (PSNR)

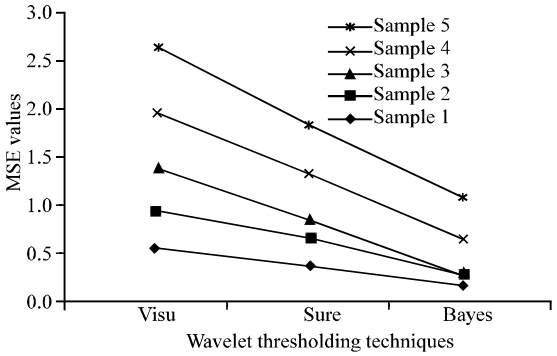

Fig. 7: Chart for Mean Square Error (MSE)

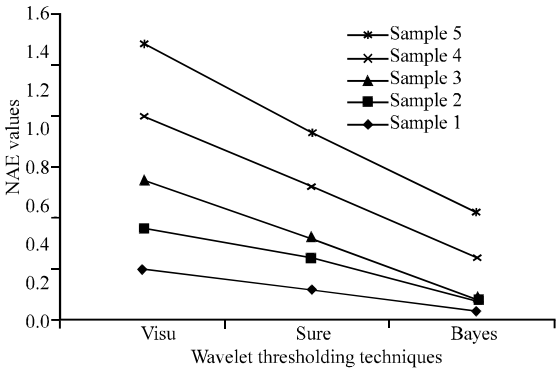

Fig. 8: Chart for Normalized Absolute Error (NAE)

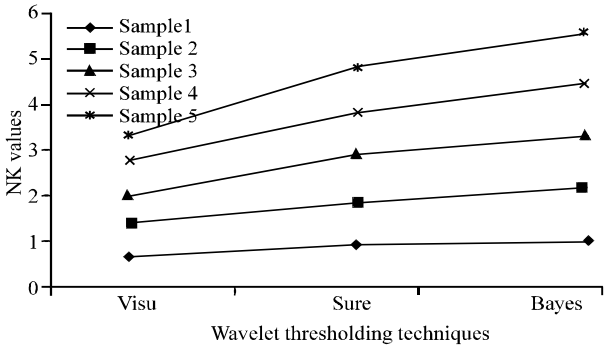

Fig. 9: Chart for Normalized cross correlation (NK)

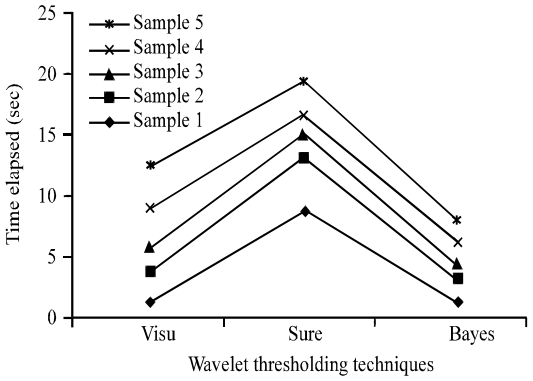

Fig. 10: Chart for time elapsed to produce denoised image

CONCLUSION

Thus, this study deals with the implementation of the three thresholding techniques in wavelet domain for denoising the brain MRI images. The inference from all these implementations are that bayes shrink performs better in terms of all performance metrics. It has high peak signal to noise ratio, lowest mean square error and lower normalized absolute error.

RECOMMENDATIONS

The future scope of this research, includes analyzing and implementing various filters for removing fBm noise while the conventional noise removal technique uses only the homomorphic filtering approach. The future scope also aims to propose a new type of filter that best suits to remove the fBm noise and to test the performance of the filters using various evaluation metrics.

REFERENCES

Al-Kadi, O.S., 2010. Assessment of texture measures susceptibility to noise in conventional and contrast enhanced computed tomography lung tumour images. Comput. Med. Imaging Graph., 34: 494-503.

Andria, G., F. Attivissimo, A.M.L. Lanzolla and M. Savino, 2013. A suitable threshold for speckle reduction in ultrasound images. IEEE Trans. Instrum. Meas., 62: 2270-2279.

Bala, E. and A. Ertuzun, 2005. A multivariate thresholding technique for image denoising using multiwavelets. EURASIP J. Applied Signal Process., 2005: 1205-1211.

Chicklore, S., V. Goh, M. Siddique, A. Roy, P.K. Marsden and G.J. Cook, 2013. Quantifying tumour heterogeneity in 18F-FDG PET/CT imaging by texture analysis. Eur. J. Nucl. Med. Mol. Imaging, 40: 133-140.

Farbiz, F., M.B. Menhaj, S.A. Motamedi and M.T. Hagan, 2000. A new fuzzy logic filter for image enhancement. IEEE Trans. Syst. Man. Cybern. B Cybern., 30: 110-119.

Gevers, T. and A.W. Smeulders, 2000. PicToSeek: Combining color and shape invariant features for image retrieval. IEEE Trans. Image Processing, 9: 102-119.

Hiremath, P.S., P.T. Akkasaligar and S. Badiger, 2013. Speckle Noise Reduction in Medical Ultrasound Images. In: Advancements and Breakthroughs in Ultrasound Images, Gunarathne, G. (Ed.). InTech Publishers, Crortia, ISBN: 978-953-51-1159-7, pp: 201-241.

Hu, J., Y. Pu, X. Wu, Y. Zhang and J. Zhou, 2012. Improved DCT-based nonlocal means filter for MR images denoising. Comput. Math. Methods Med., Vol. 2012. 10.1155/2012/232685

Le Bihan, D., 2003. Looking into the functional architecture of the brain with diffusion MRI. Nat. Rev. Neurosci., 4: 469-480.

Liu, Y., D. Zhang, G. Lu and W.Y. Ma, 2007. A survey of content-based image retrieval with high-level semantics. Pattern Recognition, 40: 262-282.

Minnie, D. and S. Srinivasan, 2014. Preprocessing and generation of association rules for bone marrow analysis data of haematology for acute myeloid leukemia. Asian J. Inform. Technol., 13: 29-37.

Oigard, T.A., L.L. Scharf and A. Hanssen, 2005. Time-frequency and dual-frequency representation of fractional Brownian motion. Proceedings of the IEEE/SP 13th Workshop on Statistical Signal Processing, July 17-20, 2005, Novosibirsk, Russia, pp: 889-894.

Penttinen, A. and J. Virtamo, 2005. Simulation of two-dimensional fractional Brownian motion. Methodol. Comput. Applied Probability, 6: 99-107.

Xu, F., T. Fan, C. Huang, X. Wang and L. Xu, 2014. Block-based MAP superresolution using feature-driven prior model. Math. Problems Eng., Vol. 2014. 10.1155/2014/508357.